Published in final edited form as:

Recent Pat Biotechnol. 2012 December ; 6(3): 172–183. doi:10.2174/1872208311206030172.

Hyperthermia: From Diagnostic and Treatments to New Discoveries

Sandra Romero-Suarez[1], **Chenglin Mo**[1], **Chad Touchberry**[2], **Nuria Lara**[3], **Kendra Baker**[1], **Robin Craig**[1], **Leticia Brotto**[1], **Jon Andresen**[2,1], **Michael Wacker**[2,1], **Simon Kaja**[4], **Eduardo Abreu**[1], **Wolfgang Dillmann**[5], **Ruben Mestril**[6], **Marco Brotto**[1,2], **Thomas Nosek**[7,*]

[1]University of Missouri-Kansas City, Muscle Biology Research Group-MUBIG, School of Nursing

[2]School of Medicine;

[3]Department of Oral Biology, School of Dentistry;

[4]Vision Research Center and Department of Ophthalmology, School of Medicine;

[5]University of California at San Diego, School of Medicine;

[6]Loyola University Chicago, Department of Cell and Molecular Physiology;

[7]Case Western Reserve University, School of Medicine

Abstract

Hyperthermia is an important approach for the treatment of several diseases. Hyperthermia is also thought to induce hypertrophy of skeletal muscles *in vitro* and *in vivo*, and has been used as a therapeutic tool for millennia. In the first part of our work, we revise several relevant patents related to the utilization of hyperthermia for the treatment and diagnostic of human diseases. In the second part, we present exciting new data on the effects of forced and natural overexpression of HSP72, using murine *in vitro* (muscle cells) and ex vivo (primary skeletal muscles) models. These studies help to demonstrate that hyperthermia effects are orchestrated by tight coupling between gene expression, protein function, and intracellular Ca^{2+} signaling pathways with a key role for calcium-induced calcium release. We hope that the review of current patents along with previous unknown information on molecular signaling pathways that underlie the hypertrophy response to hyperthermia in skeletal muscles may trigger the curiosity of scientists worldwide to explore new inventions that fully utilize hyperthermia for the treatment of muscle diseases.

Keywords

Hyperthermia; heat-shock; gene regulation; hypertrophy; Ca^{2+} homeostasis; sarcoplasmic reticulum (SR); calcium-induced calcium release (CICR); ryanodine receptor (RyR); store operated calcium entry (SOCE); muscle function; inventions; patents

*Address correspondence to this author at the Department of Physiology & Biophysics, School of Medicine, Case Western Reserve University, Cleveland, Ohio, 44105, Tel: 216-368-3443; Fax: 216-368-5586; tmn2@case.edu.

CONFLICTS OF INTEREST

The author(s) confirm that this article content has no conflicts of interest.

INTRODUCTION

Hyperthermia is an important approach for the treatment of several diseases [1, 2]. Hyperthermia is also thought to induce hypertrophy of skeletal muscles *in vitro* and *in vivo* [3], but molecular mechanisms for these effects remain elusive.

Much of the current knowledge about the effects of heat shock proteins in striated muscles is the result of pioneering studies by Mestril & Dillman in the early 1990's, which demonstrated that a specific family of HS proteins was able to protect cardiomyocytes and the heart against hypoxia, ischemia, and ischemia-reperfusion [4–7].

In the second part of this manuscript we will show tantalizing new data that suggests that the skeletal muscle cells respond to heat shock in a manner where gene/protein function is highly orchestrated with changes in intracellular calcium homeostasis. Next we will focus on a short review of some of the key patents related to hyperthermia filled in the US in the last decade.

Magnetic Resonance Guided Hyperthermia *(Issued Patent #US5492122/Button et al/Feb 20, 1996)*

This patent [8] described a hyperthermia treatment apparatus that includes an annular radio frequency (RF) antenna array with bolus that is compatible with a magnetic resonance imaging (MRI) machine. Antenna elements polarized parallel to the axis of the cylinder are used for forming a Specific Absorption Ratio (SAR) map as well as for directing the energy to accomplish hyperthermia. The array may be dynamically controlled to focus energy at any specified region within the cylinder. The array is positioned inside an MRI machine and is tuned to the machine's hydrogen resonant frequency. For treatment planning, the array is employed to form an SAR map via RF current density imaging. Using this map, array phase, amplitude, and temporal weighting are optimized until the SAR maxima is congruent with the treatment volume. For treatment, RF radiation is applied to the subject to induce heating of the treatment volume using these optimal array parameters. Temperature is periodically determined via noninvasive MRI methods. Some clinical applications have appeared of this basic idea and have been implemented. Grull and Langereis (2012, http://www.ncbi.nlm.nih.gov/pubmed/22565055) have for example recently reviewed the hyperthermia-triggered drug delivery from temperature-sensitive liposomes using MRI-guided high intensity focused ultrasound. High intensity ultrasound was a great breakthrough in the safe generation of localized tissue hyperthermia (40–45°C) and its applications range from cancer treatment to muscle injuries, particularly contusions.

Chemical Induced Intracellular Hyperthermia *(Issued Patent #US7635722/ Bachynsky et al./Jul 27, 1999)*

This invention [9] relates to therapeutic pharmacological agents and methods to chemically induce intracellular hyperthermia and/or free radicals for the diagnosis and treatment of infections, malignancy and other medical conditions. The invention also relates to a process and composition for the diagnosis or killing of cancer cells and inactivation of susceptible bacterial, parasitic, fungal, and viral pathogens by chemically generating heat, and/or free

radicals and/or hyperthermia-inducible immunogenic determinants by using mitochondrial uncoupling agents, especially 2,4 dinitrophenol and, their conjugates, either alone or in combination with other drugs, hormones, cytokines and radiation.

The basic idea underlying this and similar inventions is that hyperthermia is able to elevate the intracellular levels of heat shock proteins and oxidative stress response, which in turn might provide an enhanced fighting environment against cancer. Interesting that Patel *et al.* (http://www.ncbi.nlm.nih/gov/pubmed/22559681.) have recently developed a method where they utilized multifunctional biodegradable and biocompatible poly lactic-co-glycolic acid (PLGA) nanoparticles loaded with indocyanine green (ICG) as an optical-imaging contrast agent for cancer imaging and as a photothermal therapy agent for cancer treatment.

Apparatus for Implementing Hyperthermia *(Issued Patent #US6579496/Fausset et al. /Jun 17, 2003)*

This invention [10] was filed in 1999 and described an apparatus and system for extracorporeal treatment that utilizes a hemodialysis machine capable of heating dialysis fluid to 48°C, an optional parallel plate hemodialyzer together with a sorbent-based detoxifier, a tubular heat exchanger and a high flow pumping addition to various probes and catheters to effect extracorporeal treatment without adverse physiological effect and without the specific need for general anesthesia. The system inheres in the combined high flow of the pump-up to 2400 ml per minute and the high temperature of 52°C is achievable in the heat exchanger, which together provide unprecedented speed and efficiency in the administration of hyperthermia treatments. The system is also a potentiating system in the administration of heat sensitive pharmaceutically active agents and is particularly useful in the isolated anatomic areas of a patient. This invention has certainly evolved into very important clinical devices used particularly in cardiac intervention units in the US that maintain patients alive for periods equal or superior to 1week during which time the heart of the patient is “resting or recovering”.

Injectable Superparamagnetic Nanoparticles for Treatment by Hyperthermia and Use for Forming an Hyperthermic Implant *(Patent Application #US 20090081122/Rufenacht et al. / March 26, 2009)*

In this invention [11] authors described the creation of an injectable formulation for treatment by hyperthermia. It comprises a liquid carrier and heat-generating superparamagnetic iron oxide nanoparticles having a mean diameter not greater than 20nm. This injectable formulation is able to form in-situ a hyperthermic solid or semi-solid implant upon contact with body fluids or tissue. Said hyperthermic solid or semi-solid implant may be useful for treating a tumor or a degenerative disc disease by hyperthermia. In 2010, Renard et al reported testing the efficacy of this invention. They investigated the use of in situ implant formation that incorporates superparamagnetic iron oxide nanoparticles (SPIONs) as a form of minimally invasive treatment of cancer lesions by magnetically induced local hyperthermia. We developed injectable formulations that form gels entrapping magnetic particles into a tumor. The group used SPIONs embedded in silica microparticles to favor syringeability and incorporated the highest proportion possible to allow large heating capacities. Hydrogel, single-solvent organogel and cosolvent

(lowtoxicity hydrophilic solvent) organogel formulations were injected into human cancer tumors xenografted in mice. The thermoreversible hydrogels (poloxamer, chitosan), which accommodated 20% w/v of the magnetic microparticles, proved to be inadequate. Alginate hydrogels, however, incorporated 10% w/v of the magnetic microparticles, and the external gelation led to strong implants localizing to the tumor periphery, whereas internal gelation failed in situ. The organogel formulations, which consisted of precipitating polymers dissolved in single organic solvents, displayed various microstructures. A 8% poly(ethylene-vinyl alcohol) in DMSO containing 40% w/v of magnetic microparticles formed the most suitable implants in terms of tumor casting and heat delivery. Authors emphasized the great clinical interest to develop cosolvent formulations with up to 20% w/v of magnetic microparticles that show reduced toxicity and centered tumor implantation.

Supported Hypo/Hyperthermia Pad *(Issued Patent US6871365/Flick et al. /Mar 29, 2005)*

Authors proposed the development of a first conformable material having a three-dimensional shape and a first hypothermia and/or hyperthermia device [12]. This invention is used as a pad for sleeping, lying down, or sitting, to maintain a desired temperature to the contacting surface of a body to the pad. The conformable material is a gelatinous elastomeric material. It is very interesting to note that obviously in this case the objective was much more to alleviate pain and/or localized inflammations. The combination of heat and cold therapy in the same device is also advantageous for the treatment of sports related injuries. Interestingly that Adroit Medical System manufactures and sells a very diverse number of hypo/hyperthermia pads/devices but none of them combines both cold and heat treatments.

Recent Studies by Our Group Revealed new Insights into the Hyperthermia Response in Skeletal Muscle Cells

We had previously demonstrated that overexpressing HSP72 did not prevent skeletal muscles from fatiguing under normoxic conditions, but we did observe that muscles from HSP72 overexpressing mice were more sensitive to the effects of caffeine stimulation, suggesting that they had an enhanced calcium-induced calcium release (CICR) response [13].

Gene reprogramming is recognized as an important event in muscle cell growth and in general cells respond to protein damaging stressors by activating the “heat shock response”, which involves a rapid transient increase in a specific group of proteins known as heat shock proteins (HSPs) [14]. Heat shock protein HSP72 and HSP25 are found in cells throughout the body and are particularly abundant in nerve and muscle cells [15, 16].

Although several molecules involving stress-induced muscle hypertrophy have been proposed, the role of hyperthermia as a modulator of muscular hypertrophy remains largely unclear, with a few genes and proteins being identified as markers of the heat shock adaptation [17].

In an attempt to fill some of the gaps in our understanding of the HS response in skeletal muscles, we studied muscle contractility in the HSP72 overexpressor mice under hypoxic-fatiguing conditions that better mimics the ischemic condition in the heart where HSP72 has

been shown to be protective. Next, to provide a comprehensive and in depth analysis of the HS response, we studied this response in C2C12 cells by simultaneously analyzing genes, cell diameter and area, protein content, intracellular Ca^{2+} signaling, and key proteins that are considered to be markers of the HS adaptation response. A quantitative Real-time gene PCR approach was used to determine the expression levels of muscle specific genes involved with the HS response. Next, we tested if HS activated the stress response in myotubes cells by measuring the content of HSP72 and the levels of phosphorylated HSP25 (pHSP25) and found both to be significantly upregulated.

To further investigate cellular mechanisms, we established in C2C12 myotubes that increased cell area was correlated with higher total protein content, suggesting an increased level of protein synthesis. Ca^{2+} homeostasis regulation was examined by measuring intracellular Ca^{2+} to determine if HS can modulate intracellular Ca^{2+} homeostasis and whether such modulation might be linked to the heat shock response and adaptation. This was critical to link our reported observation that HSP72 overexpressing muscles have enhanced sensitivity to caffeine. Here, we found exactly the same response. C2C12 muscle cells acutely treated with HS demonstrated enhanced sensitivity to caffeine stimulation.

Together, our data pointed to intracellular calcium modifications as a key process in muscle adaptation to HS in both animal and cell models. To link these changes with the detected cellular hypertrophy in C2C12 muscle cells, we measured the content of NFATc3, a downstream protein that is key marker for the activation of the Ca^{2+}/Calcineurin pathway, and fundamental for the hypertrophic response in skeletal muscles, and we found a substantial 10-fold increase in the content of this downstream protein that is also a key marker of cellular hypertrophy. These findings are physiologically relevant because activation of the Ca^{2+}/Calcineurin pathway necessarily involve modulation of intracellular calcium homeostasis, and a hallmark of both muscles from HSP72 overexpressor mice and C2C12 acutely overexpressing HSP72 was precisely the enhancement of CICR. Furthermore, this critical change was supported by upregulation of genes involved with modulation of CICR.

This study offers important new information into the functional and biochemical adaptations that occur in both *in vivo* and *in vitro* mammalian models that might help shed some light into the effects of hyperthermia on skeletal muscles. Our studies also provide the initial evidence of a complex network of genes and proteins working in concert with Ca^{2+} signaling mechanisms to modulate myotube growth in response to HS. Learning to utilize and modulate these pathways could be important for the development of therapies for skeletal muscle diseases characterized by muscle wasting.

EXPERIMENTAL PROCEDURES

Animal Model

Transgenic B6 3 SJL mice developed by Dillmann and Mestril [6], were produced using a chimeric transgene consisting of a rat inducible HSP72 inserted into the vector pCAGGS. Transgene-negative, wild-type (WT), littermate mice were used as controls. Care was taken to ensure that all procedures relating to the living animals were in accordance

with the “Guiding Principles in the Care and Use of Animals” approved by the American Physiological Society and the University of Missouri-Kansas City.

Intact Muscle Preparation

The detailed experimental protocol for isolation of intact muscle from mice has been previously demonstrated [13, 18] as well as the conditions to produce experimental hypoxia where the levels of dissolved O_2 in the experimental chamber were ~40 mmHg [19, 20]. Briefly, the mice were euthanized by CO_2 inhalation, pairs of intact extensor digitorum longus (EDL) and soleus (SOL) muscles were dissected from transgenic and littermate control animals, immediately placed on a dish containing a modified HEPES-Ringer solution (142 mM NaCl, 5 mM KCl, 2.5 mM $CaCl_2$, 1.8m M $MgCl_2$, 5mM HEPES, and 10mM glucose at pH 7.35), and continuously aerated with 100% O_2 until mounted. The muscles were mounted vertically on two Radnoti (Monrovia, CA) glass apparati with platinum stimulating electrodes, each muscle end attached to an isometric force transducer or to the stationary post of the stimulating apparatus, and immersed in a 20-ml bathing chamber containing the aerated HEPES-Ringer solution described above.

Stimulation Protocols

The muscles were then subjected to several frequencies of stimulation ranging from 1 to 140 Hz (300mA, train duration of 500ms, single stimulation pulses of 1ms) to produce the force-frequency relationship. The frequencies at which maximum isometric tetanic force, T_{max} (100–120Hz for EDL and 70–90Hz for SOL) and 50% T_{max} (50–70Hz for EDL and 30–40Hz for SOL) were used in the entire protocol. Briefly, muscles were stimulated with alternating frequencies producing T_{max} and 50% T_{max} with a periodicity of 1min during equilibration with O_2, equilibration with N_2, and all the recovery period, while with a periodicity of 1sec during the fatigue protocol (See Fig. 1A–B for details). To follow the time course and recovery from fatiguing stimulation, all force data were normalized to the T_{max} event measured just prior to the start of the hypoxia (EO_2 time point in Fig. 1A–B). The entire experiment was controlled by PowerLab system (ADInstruments, Inc, Coloarado Springs, CO) and the output of the force transducer was digitized and stored in a computer and was analyzed with PowerLab software. All experiments were performed at room temperature (22–24°C).

Determination of Oxygen Tension, PO2 and Experimental Hypoxia

Values of PO_2 were determined using a microelectrode system (DO-166NP, Lazar Research Laboratories, Los Angeles, CA) that measures dissolved oxygen directly from solutions, tissues and other biological samples without involving the titrations needed with the Winkler method [19, 20]. We also performed these experiments using a HEPES and not bicarbonate based buffer to assure that the only variable undergoing a change would be PO_2 and not the Ringer’s pH. During the last 10 min of the equilibration period, while the periodicity of the electrical pulse trains was maintained, O_2 was substituted by 100% N2 that produced a PO_2=40±5 mmHg (≅ 5 kPa) compared to 250±10 mm Hg (≅ 33 kPa) in the control groups (see Fig. 1). These levels of 40 mmHg PO_2 were used during the hypoxia, hypoxia-fatigue, and the recovery under hypoxia, while the levels of 250mmHg were used during the initial

phase of the equilibration, the recovery periods with oxygen and also during the addition of caffeine.

Normalization of Data

T_{max} was normalized to either 100% or as the force/cross sectional area, as previously described [19], by using the following relationship: F/CSA=(F × L × 1.06)/m, where F is force in grams, CSA is cross-sectional area in cm^2, L is muscle length in cm and m is muscle mass in grams, and 1.06 represents the density of the muscle in kg/l. To follow the time course and recovery from fatiguing stimulation, all force data were normalized to the single high-frequency tetanic force measured just prior to the fatiguing protocol. Force vs. frequency data were normalized to the maximum force generated by each muscle. The numbers of muscle preparations used in this study were 10 for both transgenic and littermate controls.

Cell Models

C2C12 myoblasts and myotubes were cultured as previously described [21]. Fully differentiated myotubes were placed in a water bath at 43°C for 20 minutes. The cell pellets were collected and frozen at −80°C until a specific series of experiments was performed. The effects of HS were independent of the confluence levels of myotubes.

RNA Extraction and cDNA Synthesis

Total RNA was extracted from the myotubes using a standard trizol-based extraction method (Sigma Aldrich, St. Louis, MO), quantified in a Nanodrop spectrophotometer (Thermo Scientific, Wilmington, DE) by determining absorbance at 260nm in triplicates. RNA purity was indicated by the A260/280 nm absorbance ratio of 1.9–2.1. Using 1 μg/μl of RNA, each sample was reverse transcribed in a 20μl reaction volume with a commercial Quantitec Reverse Transcription Reagents kit (Qiagen Inc, Valencia, CA) according to the manufacturer's instructions.

Assessment of RNA Yield and Quality

C2C12 cells collection and storage were optimized to guarantee the maximum yield of RNA. To prevent RNA degradation, cells RNA extraction was performed using RNase-free materials and solutions. Protein contamination was assessed by the 260/280 ratio in a Nanovue Plus spectrophotometer (GE Healthcare, Piscataway, NJ). The average purity was 1.92±0.23 (n=4), indicating high-quality RNA. The expression of 96 genes of interest was investigated using a customized Mouse RT^2 Profiler™ PCR Array system (SABiosciences, Qiagen, Inc., Valencia, CA). Genes were grouped into 5 main groups: heat shock/stress, survival and metabolic, Ca^{2+} signaling, Ca^{2+} release, and hypertrophy genes. The expression of these genes was determined at 4 experimental time points after HS (20 min, 1 h, 2 h, and 24 h). qPCR was performed using the Step-OnePlus ™ Real-Time PCR System (ABI, Foster City, CA, USA) via standard fluorescent methodology and thermal cycling conditions following the manufacture's recommendations, including a threshold of 0.2 and validation of each gene tested by the identification of single peaks in melting curves. The real-time PCR reaction mixture contained 1μl of 50 ng of cDNA, 12.5 μl of the RT^2 Real-Time ™

SYBR Green/Rox PCR master mix, 1 μl of primer pairs and 10.5 l of RNase free water to a complete reaction of 25 μl. Data was analyzed using RT^2 Profiler™ PCR Array software, and relative amounts were calculated by the $2^{-\Delta\Delta CT}$ method [22]. C_T values of the genes were normalized to GAPDH. Gene expression was determined as up/down regulation of the gene of interest compared to the control.

Expression Levels of the Candidate Reference Genes

We investigated the expression levels and variability for five candidate reference genes (*B2m, GAPDH, Hprt1, Rplp1* and *Actb*), both for normal and HS conditions. C_T values from GAPDH showed an average of 0.3 cycle difference and an efficiency of 94%; therefore, this gene was selected for normalization purposes.

Total Protein

HS-treated myotubes were washed three times with PBS and lysed with RIPA Cell extraction buffer (Sigma Aldrich, St. Louis, MO) supplemented with a cocktail of protease and phosphatase inhibitors (Sigma Aldrich, St. Louis, MO). The protein concentrations were quantified using the Micro BCA Protein assay Kit (Pierce, Thermo Fisher Scientific, Rockford, IL) with BSA as standards and quantified by optical density at 562 nm using a Bio-TEK micro-plate reader. These experiments were repeated 4 times and performed in triplicates.

Cell Area

C2C12 myotubes were imaged using a Leica DM 4000B (Leica Microsystems Inc, Buffalo Grove, IL) microscope. Diameters and areas of individual cells were determined using the Leica Application Suite Advanced Imaging and Fluorescence software package (Leica Microsystems Inc, Buffalo Grove, IL) by defining cells as regions of interest, and then areas were automatically calculated in micrometers squared (μm^2) by the Leica software.

Intracellular Ca^{2+}

A Photon Technology International (PTI, Birmingham, NJ) imaging system was used to measure intracellular Ca^{2+} homeostasis as previously described by our group [23]. Briefly, fully differentiated C2C12 myotubes were loaded with 2 μM Fura-2-AM for 30 minutes at 37°C. After this loading period, Fura-2-AM was washed off and allowed to de-esterify at room temperature for 15 min. An automatic wavelength (0–650 nm) PTI photometer system was used to determine the magnitude and kinetic changes of caffeine-induced intracellular Ca^{2+} transients reported as the relative ratio of 350/375 nm emitted at 510 nm. The excitation pair (350/375 nm) was determined as the optimal wavelength pair under our experimental conditions by using the scanning spectral properties of our Ca^{2+} imaging system. Under our experimental conditions each 0.1 units of ratio change equaled approximately 125nM of cytoplasmic Ca^{2+} concentration $[Ca^{2+}]_i$. Fully differentiated myotubes had a resting level of Ca^{2+} of ~120nM and in response to 10mM caffeine, the magnitude of peak of the Ca^{2+} transient reached to approximately 1μM $[Ca^{2+}]_i$.

Western Blot Analysis

The expression levels of HSP72, pHSP25 and NFATc3 in HS-treated and control C2C12 myotubes were determined as modified from Zhao *et al.* [21]. 40 μg of total protein were separated using a gradient gel of 4–10, 10–20 and 15% SDS polyacrylamide gel electrophoresis (PAGE), and electrophoretically transferred to a PVDF membrane (Amersham International, Amersham, UK) using the Bio-Rad Mini-Protean II gel transfer system. Blots were probed with polyclonal antibodies (#SPA-800, #SPA-810; Stress-Gen, Ann Harbor, MI, SC-8321 Santa Cruz Biotechnology, Inc, Santa Cruz, CA) specific for HSP72, pHSP25, and NFATc3, respectively, diluted in 0.1% TBST (0.1 M tris-buffered saline, 0.1% Tween 20) containing 0.3% BSA and then incubated overnight at 4°C at constant shaking conditions. The membranes were rinsed 3 times for 5 min in 0.1% TBST before incubation for 1h with a horseradish peroxidase-labeled conjugated secondary antibody (#SAB-100 Stress-Gen, Ann Harbor, MI). The immunoreactive bands were detected using an enhanced chemiluminescence kit (Pierce, Thermo Fisher Scientific, Rockford, IL). The chemiluminecent signal on the membrane was scanned using ImageQuant™ RT-ECL (GE Healthcare, Piscataway, NJ). Immunoblots were visualized and the intensities of the bands of interest were quantified using the AlphaEaseFC densitometry software (Alpha Innotech, San Leandro, CA). The reference protein GAPDH was used as internal loading control for western blot analysis. The content was expressed as the relative ratio [%] to their own controls.

Statistical Analysis

All graphs were made and statistical procedures were performed using ORIGIN 6.1 Scientific Graphing and Data Analysis Software (OriginLab Corp, Northampton, MA). Data are expressed as mean ± S.D. Data were compared either with paired *t* tests or ANOVA, followed by Tukey's test, with significance set at the $p<0.05$ level.

RESULTS

The Tension vs. Time relationships of the *ex-vivo*, intact muscles from transgenic HSP72 overexpressor (TG) and control mice (WT) are shown in (Fig. 1A (EDL) and 1B) (Soleus). In general, HSP72 overexpressing muscles fatigued less and displayed significant improved recovery after fatigue, particularly in the presence of caffeine, suggesting enhanced response to CICR. The expression of 96 genes grouped by heat shock/stress, survival and metabolic, Ca^{2+} signaling, Ca^{2+} release, and hypertrophy genes is shown in Table 1. The expression of these genes was determined at 4 experimental time points after HS and Table 1 shows the complexity of the response over the time period studied. Our Real-time gene PCR arrays also showed the activation of *Srf, Ppp3r2, Irf, Sod3 and Pck1*, key genes involved with metabolic demand and cell survival. As shown in (Fig. 2), to determine the effects of HS on cell volume as an indication of cellular hypertrophy, we measured both cell area and total protein levels. We found that the cell area of HS treated C2C12 myoblasts increased by 38% and total protein levels by 10% in relation to control cells. These results were further supported by western blotting studies that revealed significant increases in the content of HSP72 (Fig. 3A–B) and phosphorylation levels of HSP25 (Fig. 3A–C). Final evidence that these cells were experiencing growth process (cellular hypertrophy) was

demonstrated by the 10-fold increase in the content of NFATc3 (Fig. 3D). To functionally link our aforementioned findings with the regulation of intracellular calcium homeostasis, we performed a series of experiments to measure resting levels of calcium as well as calcium transients in response to caffeine. A remarkable feature of the HS response was the enhancement of the calcium release process from the sarcoplasmic reticulum (SR), particularly via the CICR mechanism (Fig. 4).

DISCUSSION

An understanding of the roles of key proteins and genes that regulate the HS response and its potential involvement with intracellular calcium homeostasis, hypertrophy, and contractile function is crucial to the development of novel strategies for modulating muscle mass and for the improvement of muscle strength for conditions such as sarcopenia, aging frailty, muscle myopathies, and specific pathological conditions that might predispose to skeletal muscle fatigue, such as cardiovascular diseases [24].

Cardiac muscle and cardiomyocytes from the HSP72 overexpressor mouse model have been shown to be protected against the damaging effects of hypoxia and ischemia [4, 25]. Surprisingly, we previously reported that skeletal muscles from this mouse model were not protected against the effects of fatiguing stimulation [13]. A caveat of our initial studies was that muscles were fatigued under conditions of high oxygen content [13]. It has been argued that physiological fatigue does occur under hypoxic conditions [19, 20, 26–28].

In addition, since HSP72 is protective under these types of conditions in both cardiac cells and the heart, we studied here whether HSP70 could have the same protective effects in skeletal muscles under similar conditions, in that, muscles were fatigued under hypoxia. (Fig. 1A–B) shows our exciting new results demonstrating that when ex-vivo, intact EDL and SOL muscles from HSP72 overexpressor mice are fatigued under hypoxia [hypoxia-fatigue], these muscles display lesser fatigability and improved recovery after fatigue in the absence and in the presence of caffeine. These results also confirm our previous findings that HSP72 overexpressing muscles are more sensitive to caffeine [13]. While these ex-vivo contractility experiments are very important in revealing phenotypic changes, deriving mechanistic insights from them is rather difficult. To overcome this limitation we employed biophysical, biochemical and molecular approaches in the very robust C2C12 myogenic cell model. We found that the HS response was tightly regulated in C2C12 muscle cells, as demonstrated by the concomitant upregulation of *Hsp70* and *Hsp90* expression, as well as other essential genes generally considered to be markers of hypertrophy and critical for reorganization of the contractile apparatus (*Mhy7, NF-B1, Irf, Pck1*). Our Real-time gene PCR arrays also showed the activation of *Srf, Ppp3r2, Irf, Sod3 and Pck1*, key genes involved with metabolic demand and cell survival as shown in Table 1.

Morphologically, the substantial increase in cell area by 38.87±6.14% in C2C12 myotubes (Fig. 2A–C), was biochemically supported by an increased content of total protein by 10% as shown in (Fig. 2D). In addition, as shown in (Fig. 3), after 24 h of being subjected to HS, muscle cells displayed an increased content in HSP72 (3.5-fold; $P<0.001$, (Fig. 3B) and enhanced phosphorylation of HSP25 (2.3-fold; $P<0.01$, (Fig. 3C). These results clearly

show that HS activate mechanisms of the stress response orchestrated by HSP, both at the content and posttranslational levels. Final evidence that these cells were experiencing growth process (cellular hypertrophy) was demonstrated by the 10-fold increase in the content of NFATc3 (Fig. 3D). These results are in agreement with previous studies [29–32] demonstrating a role of NFATc3 in striated muscle differentiation, growth, and hypertrophy.

Heat shock factors activation and induction are relatively rapid events and known to trigger the activation of the Ca^{2+}-dependent/Calcineurin pathway that usually occur within minutes after the onset of stress and generally last for only a few hours [33]. For instance, the expression of *Hsp72* occurred rapidly and increased during the first 2h following HS. Although it was not our goal to necessarily link the HS response with the inflammatory response, HS treatment led to a transient seven-fold increase in *NF-kB1* expression at 20 minutes with expression levels going back to baseline at 1 hour. Interestingly, this result differ from other findings reported in the literature, where HS treatment has been shown to suppress the angiotensin II-induced activation of NF-kB [34], a transcription factor that controls inflammatory genes [35]. In addition, heat stress [and consequently increased HSP production] has been shown to prevent the activation of NF-kB in squamous cell carcinoma [36]. However, additional evidence that an early (20 min) inflammatory response might work as initiator of HS adaptation is the upregulation of *Irak1*, a gene that is partially responsible for IL1-induced upregulation of the transcription factor NF-kB, and *Traf-6*, an E3 ubiquitin ligase that leads to the activation of NF-kB (see Table 1).

Calcium is fundamental for both muscle contractility and hypertrophic adaptation. Fura-2 was used as the intracellular Ca^{2+} indicator and cells were challenged with 10 mM caffeine, an agent that effectively releases Ca^{2+} from the SR of skeletal muscles with the goal to establish the essential Ca^{2+} release/uptake properties of these cells. Our first observation was that the resting ratio of Fura-2 was 23% higher in HS treated cells (0.51 ± 0.05 in control myotubes vs. 0.63 ± 0.07 in HS treated myotubes, $p<0.05$, $n=10$). In addition, we found that while the peak response to caffeine was smaller in HS cells (1.27 ± 0.05 in control myotubes vs. 1.18 ± 0.05 in HS treated myotubes, $p<0.05$, $n=10$), Ca^{2+} re-uptake and extrusion mechanisms were improved as demonstrated by a faster and more efficient clearance of Ca^{2+} and establishment of lower resting levels of Ca^{2+} after exposure to caffeine (Fig. 4A–B, 4E–F). Further, a noticeable secondary peak after caffeine exposure was presented, suggesting enhancement of the Ca^{2+}-induced Ca^{2+} release (CICR) mechanism (Fig. 4A–B), or possibly entry of Ca^{2+} from the extracellular space, via store-operated Ca^{2+} entry (SOCE) for example. In search for a time line for the Ca^{2+} homeostasis changes we also monitored intracellular Ca^{2+} 1h and 2h after HS. As shown in (Figs. 4C–D), during these early time points we observed a very different pattern of response of C2C12 myotubes to caffeine. The response to caffeine was initially delayed but followed by small oscillatory and self-paced Ca^{2+} transients. In the majority of these cells, we also observed spontaneous Ca^{2+} transients and muscle cell contractions (recorded as downward deflections in our system) were also common (See Fig. 4C–D). This is an important finding and suggests a tight coupling between the HS response and intracellular Ca^{2+} homeostasis modifications, in agreement with the concept that activation of hypertrophy response genes is initiated by modifications in Ca^{2+} homeostasis and the subsequent expression of a large number of genes and synthesis of proteins involved in intracellular Ca^{2+} homeostasis and Ca^{2+} signaling [37].

We found that as early as 1 h after HS, modifications in intracellular Ca^{2+} homeostasis were closely associated with upregulation of Ca^{2+} release genes (Table 1). Interestingly, *Orai3* showed a fast expression response shortly after HS. The role of *Orai3* in skeletal muscle is currently unknown, while *Orai1* has been implicated in the modulation of SOCE in skeletal muscles during development (myogenesis/ differentiation) and also during muscle fatigue and muscle aging [21, 38]. Interestingly, *Orai3* upregulation occurred in conjunction with robust upregulation of *Jph1*, a protein needed to stabilize the junctional sarcolemma and sarcoplasmic reticulum membranes complexes which are required for proper function of excitation-contraction coupling mechanism [39]. In fact, *Jph1* is critical for proper functioning of SOCE in skeletal muscles [39]. Thus, it is feasible to speculate that *Orai3* and *Jph1* might play yet unrealized roles in the modulation of extracellular Ca^{2+} entry in skeletal muscles subjected or adapting to HS, and perhaps other forms of stress. Intriguingly, *Stim1* was downregulated during all time points investigated in our study. While this finding might be contradictory with the observed increases in the expression of *Orai3*, a recent report has demonstrated that extracellular Ca^{2+} entry via SOCE can be activated without the interaction of Stim-Orai [40]. Furthermore, since Orai1-Stim1 interaction is critical for maintenance of normal contractility [21, 38], it is possible that muscle cells utilize an alternative pathway to activate cell growth and hypertrophy in response to HS. Yet another possibility is that the overexpression of *Orai3* naturally leads to a downregulation of *Orai1* to prevent Ca^{2+} overload and dysfunctional Ca^{2+} homeostasis.

The importance of Ca^{2+} regulatory mechanisms to the overall adaptation to HS was further demonstrated in (Fig. 4), since our results suggested enhancement of the CICR response in C2C12 myotubes 1, 2, and 24h after HS. The presence of a secondary peak in response to caffeine 24h after HS and the oscillatory, self-paced Ca^{2+} transients in response to caffeine along with the spontaneous Ca^{2+} transients observed at 1 and 2h after HS are suggestive that Ca^{2+} release is not only altered but likely driven by CICR under these experimental conditions. This is very interesting as CICR is normally under voltage control in skeletal muscles. Thus, by removing the normal CICR inhibition, this specific pool of Ca^{2+} might be used for gene regulation and adaption to the overall cellular growth in response to HS. Furthermore, upregulation of inositol-1,4,5-trisphosphate receptors receptors (IP_3Rs) might help explain the enhanced CICR activity found in C2C12 cells after HS, since IP_3Rs are more sensitive to CICR than RyRs. The increased resting levels of Ca^{2+} would therefore provide the ideal environment for stimulation of CICR via IP_3Rs, and perhaps provide the oscillatory Ca^{2+} movement needed for gene modulation. Thus, it seemed logical our finding that the magnitude of the response to caffeine was reduced and cells after HS, perchance as a result of increased SR leakiness due to enhanced CICR, or the downregulation of RyR1, since caffeine is a direct agonist of the RyR1 [41].

The tight activation and regulation of these complex mechanisms that regulate the Ca^{2+} homeostasis-hypertrophic response are further supported by our findings that *Srf*, a serum response factor that is crucial for regulating contractile apparatus gene expression and sarcomeric integrity during skeletal muscle growth was upregulated 2h after HS. This factor is known to act by modulating intracellular Ca^{2+} levels [42], providing additional evidence of the tight relationship between Ca^{2+} signaling, and cell growth after HS.

We also found that genes involved with a higher metabolic demand and oxidative stress response, such as: *Sod3*, *Irak*, *Traf6* and *NF-κB1* were upregulated 20 min after HS. These studies allowed us to infer the existence of a previously undiscovered pathway related to muscle cell growth. *Irak* is responsible for *IL-1*-induced upregulation of *NF-κB1* transcription; *Traf-6* is the signal transducer in the *NF-κB1* pathway, and *NF-κB1* is a transcription factor that is activated by various intraand extracellular stimuli such as cytokines or oxidant-free radicals, which in turn are linked to cell protection from oxidative stress, and prohypertrophic response [43]. Further, upregulation of *Irf1*, an important marker of cell defense against inflammatory cytokines and *MyH7*, a gene normally found in cardiac myocytes and in type 1 skeletal muscle [slow twitch, oxidative fibers], suggested both cell growth and adaptation to oxidative stress after HS, changes that are likely orchestrated by NFATc3. Finally, *PCK1* a master regulator of gluconeogenesis was also shown to be activated by HS. The cytosolic enzyme encoded by this gene, along with GTP, catalyzes the formation of phosphoenolpyruvate from oxaloacetate, with the release of carbon dioxide and GDP. The expression of *PCK1* is known to be regulated by insulin, glucocorticoids, glucagon, cAMP, and diet [44]. To our knowledge, our work is the first one to demonstrate that HS upregulates *PCK1* expression suggesting that the cell growth adaptation produced by HS requires glucose from non-carbohydrate sources (e.g., lactate, glycerol, and glucogenic aminoacids) [45]. It is plausible to conclude that the molecular trigger for *PCK1* upregulation could be increased levels of cAMP from activation of the Ca^{2+}/Calcineurin-NFATc3 pathway.

These studies in the C2C12 cell line when looked in light of our animal model results might offer a feasible explanation for the enhancement performance of skeletal muscles overexpressing HSP72. The enhancement in CICR function along with gene adaptations that favor oxidative pathways could provide a quite logical explanation for the phenotypic changes of HSP72 overexpressing muscles.

CONCLUSIONS

In conclusion, our studies offer important new information on the molecular pathway involved with HS-induced cellular growth in both an established transgenic model of HSP72 upregulation and a robust model of a mammalian myogenic cell line where acute HS induced significant upregulation of HSP72. A tightly regulated mechanism involving Ca^{2+} homeostasis and gene/protein functions underlies the coordinated response of C2C12 muscle cells to hyperthermia and the resulting cellular growth. Similar mechanisms seem to be important for the improved muscle function observed in HSP72 overexpresor mice. Exploring this new information for drug and supplement targeting in skeletal muscles could prove useful.

CURRENT AND FUTURE DEVELOPMENTS

Understanding of the signaling pathways regulating the hyperthermia response in skeletal muscles might be helpful for the development of therapies to counteract muscle wasting diseases such as muscle myopathies and aging sarcopenia. Current patents have not capitalized yet on some of these advancements of our bench knowledge. In a recent series

of experiments, we have also found that HS promotes significant cellular hypertrophy of murine cardiac cells and rat AR-75 smooth muscle cells, suggesting a conserved mechanism in different muscle types from different species to the HS. Hopefully, these new studies and new combined knowledge on hyperthermia will lead to enough scientific inquiry which will lead to the development of new patents to explore these molecular mechanisms for the treatment of human diseases.

ACKNOWLEDGEMENTS

This work was supported by a Grand Opportunity (GO) NIH-NIAMS grant 1RC2AR058962-01, an American Heart Association grant 0535555N; and two Missouri Life Sciences Research Board Grants to M.B. and an USAMRMC grant to RM. We would also like to acknowledge the help of Mr. Todd Hall with the intracellular calcium measurements.

REFERENCES

[1]. Moyer HR, Delman KA. The role of hyperthermia in optimizing tumor response to regional therapy. Int J Hyperthermia. 2008 May;24(3):251–61. [PubMed: 18393003]

[2]. Wust P, Gellermann J, Rau B, Loffel J, Speidel A, Stahl H, et al. Hyperthermia in the multimodal therapy of advanced rectal carcinomas. Recent Results Cancer Res. 1996;142:281–309. [PubMed: 8893348]

[3]. Goto K, Oda H, Kondo H, Igaki M, Suzuki A, Tsuchiya S, et al. Responses of muscle mass, strength and gene transcripts to longterm heat stress in healthy human subjects. Eur J Appl Physiol. 2011 Jan;111(1):17–27. [PubMed: 20803152]

[4]. Iwaki K, Chi SH, Dillmann WH, Mestril R. Induction of HSP70 in cultured rat neonatal cardiomyocytes by hypoxia and metabolic stress. Circulation. 1993 Jun;87(6):2023–32. [PubMed: 8504517]

[5]. Mestril R, Chi SH, Sayen MR, O'Reilly K, Dillmann WH. Expression of inducible stress protein 70 in rat heart myogenic cells confers protection against simulated ischemia-induced injury. J Clin Invest. 1994 Feb;93(2):759–67. [PubMed: 8113409]

[6]. Dillmann WH, Mestril R. Heat shock proteins in myocardial stress. Z Kardiol. 1995;84 Suppl 4:87–90. [PubMed: 8585278]

[7]. Martin JL, Mestril R, Hilal-Dandan R, Brunton LL, Dillmann WH. Small heat shock proteins and protection against ischemic injury in cardiac myocytes. Circulation. 1997 Dec 16;96(12):4343–8. [PubMed: 9416902]

[8]. Button T, Barbour S, Cermignani J, Crugnale E, McGill R, Spacht G: Magnetic resonance guided hyperthermia. US5492122 (1996).

[9]. Bachynsky N, Roy W: Chemical induced intracellular hyperthermia.US7635722 (1999).

[10]. Fausset M, Keeling G, Clupper M, Rainier B: Apparatus for implementing hyperthermia.US6579496 (2003).

[11]. Rufenacht D, Doelker E, Jordan O, Chastellain M, Petri-Fink A, Hofmann H: Injectable superparamagnetic nanoparticles for treatment by hyperthermia and use for forming an hyperthermic implant.US20090081122 (2009).

[12]. Flick R, Jusiak J: Supported hypo/hyperthermia pad. US6871365 (2005).

[13]. Nosek TM, Brotto MA, Essig DA, Mestril R, Conover RC, Dillmann WH, et al. Functional properties of skeletal muscle from transgenic animals with upregulated heat shock protein 70. Physiol Genomics. 2000 Nov 9;4(1):25–33. [PubMed: 11074010]

[14]. Kregel KC. Heat shock proteins: modifying factors in physiological stress responses and acquired thermotolerance. J Appl Physiol. 2002 May;92(5):2177–86. [PubMed: 11960972]

[15]. Inaguma Y, Goto S, Shinohara H, Hasegawa K, Ohshima K, Kato K. Physiological and pathological changes in levels of the two small stress proteins, HSP27 and alpha B crystallin, in rat hindlimb muscles. J Biochem. 1993 Sep;114(3):378–84. [PubMed: 8282729]

[16]. Huey KA. Regulation of HSP25 expression and phosphorylation in functionally overloaded rat plantaris and soleus muscles. J Appl Physiol. 2006 Feb;100(2):451–6. [PubMed: 16223977]

[17]. Fluck M, Hoppeler H. Molecular basis of skeletal muscle plasticity--from gene to form and function. Rev Physiol Biochem Pharmacol. 2003;146:159–216. [PubMed: 12605307]

[18]. Brotto MA, Nagaraj RY, Brotto LS, Takeshima H, Ma JJ, Nosek TM. Defective maintenance of intracellular Ca2+ homeostasis is linked to increased muscle fatigability in the MG29 null mice. Cell Res. 2004 Oct;14(5):373–8. [PubMed: 15538969]

[19]. Brotto MA, Andreatta-van Leyen S, Nosek CM, Brotto LS, Nosek TM. Hypoxia and fatigue-induced modification of function and proteins in intact and skinned murine diaphragm muscle. Pflugers Arch. 2000 Sep;440(5):727–34. [PubMed: 11007314]

[20]. de Paula Brotto M, van Leyen SA, Brotto LS, Jin JP, Nosek CM, Nosek TM. Hypoxia/fatigue-induced degradation of troponin I and troponin C: new insights into physiologic muscle fatigue. Pflugers Arch. 2001 Aug;442(5):738–44. [PubMed: 11512030]

[21]. Zhao X, Weisleder N, Thornton A, Oppong Y, Campbell R, Ma J, et al. Compromised store-operated Ca2+ entry in aged skeletal muscle. Aging Cell. 2008 Aug;7(4):561–8. [PubMed: 18505477]

[22]. Livak KJ, Schmittgen TD. Analysis of relative gene expression data using real-time quantitative PCR and the 2(-Delta Delta C(T)) Method. Methods. 2001 Dec;25(4):402–8. [PubMed: 11846609]

[23]. Romero-Suarez S, Shen J, Brotto L, Hall T, Mo C, Valdivia HH, et al. Muscle-specific inositide phosphatase (MIP/MTMR14) is reduced with age and its loss accelerates skeletal muscle aging process by altering calcium homeostasis. Aging (Albany NY). 2010 Aug;2(8):504–13. [PubMed: 20817957]

[24]. Andersson DC, Marks AR. Fixing ryanodine receptor Ca leak - a novel therapeutic strategy for contractile failure in heart and skeletal muscle. Drug Discov Today Dis Mech. 2010 Summer;7(2):e151–e7. [PubMed: 21113427]

[25]. Marber MS, Mestril R, Chi SH, Sayen MR, Yellon DM, Dillmann WH. Overexpression of the rat inducible 70-kD heat stress protein in a transgenic mouse increases the resistance of the heart to ischemic injury. J Clin Invest. 1995 Apr;95(4):1446–56. [PubMed: 7706448]

[26]. Babcock MA, Johnson BD, Pegelow DF, Suman OE, Griffin D, Dempsey JA. Hypoxic effects on exercise-induced diaphragmatic fatigue in normal healthy humans. J Appl Physiol. 1995 Jan;78(1):82–92. [PubMed: 7713848]

[27]. Heunks LM, Machiels HA, de Abreu R, Zhu XP, van der Heijden HF, Dekhuijzen PN. Free radicals in hypoxic rat diaphragm contractility: no role for xanthine oxidase. Am J Physiol Lung Cell Mol Physiol. 2001 Dec;281(6):L1402–12. [PubMed: 11704536]

[28]. Hodgson DR, Rose RJ, Kelso TB, McCutcheon LJ, Bayly WM, Gollnick PD. Respiratory and metabolic responses in the horse during moderate and heavy exercise. Pflugers Arch. 1990 Sep;417(1):73–8. [PubMed: 2293204]

[29]. Michel RN, Dunn SE, Chin ER. Calcineurin and skeletal muscle growth. Proc Nutr Soc. 2004 May;63(2):341–9. [PubMed: 15294053]

[30]. Michel RN, Chin ER, Chakkalakal JV, Eibl JK, Jasmin BJ. Ca2+/calmodulin-based signalling in the regulation of the muscle fibre phenotype and its therapeutic potential via modulation of utrophin A and myostatin expression. Appl Physiol Nutr Metab. 2007 Oct;32(5):921–9. [PubMed: 18059617]

[31]. Kobayashi T, Goto K, Kojima A, Akema T, Uehara K, Aoki H, et al. Possible role of calcineurin in heating-related increase of rat muscle mass. Biochem Biophys Res Commun. 2005 Jun 17;331(4):1301–9. [PubMed: 15883017]

[32]. Sakuma K, Yamaguchi A. The functional role of calcineurin in hypertrophy, regeneration, and disorders of skeletal muscle. J Biomed Biotechnol. 2010;2010:721219. [PubMed: 20379369]

[33]. Locke M Heat shock protein accumulation and heat shock transcription factor activation in rat skeletal muscle during compensatory hypertrophy. Acta Physiol (Oxf). 2008 Mar;192(3):403–11. [PubMed: 17973955]

[34]. Chen Y, Arrigo AP, Currie RW. Heat shock treatment suppresses angiotensin II-induced activation of NF-kappaB pathway and heart inflammation: a role for IKK depletion by heat shock? Am J Physiol Heart Circ Physiol. 2004 Sep;287(3):H1104–14. [PubMed: 15087290]

[35]. Chen Y, Ross BM, Currie RW. Heat shock treatment protects against angiotensin II-induced hypertension and inflammation in aorta. Cell Stress Chaperones. 2004 Mar;9(1):99–107. [PubMed: 15270082]

[36]. King TA, Ghazaleh RA, Juhn SK, Adams GL, Ondrey FG. Induction of heat shock protein 70 inhibits NF-kappa-B in squamous cell carcinoma. Otolaryngol Head Neck Surg. 2005 Jul;133(1):70–9. [PubMed: 16025056]

[37]. Berchtold MW, Brinkmeier H, Muntener M. Calcium ion in skeletal muscle: its crucial role for muscle function, plasticity, and disease. Physiol Rev. 2000 Jul;80(3):1215–65. [PubMed: 10893434]

[38]. Stiber J, Hawkins A, Zhang ZS, Wang S, Burch J, Graham V, et al. STIM1 signalling controls store-operated calcium entry required for development and contractile function in skeletal muscle. Nat Cell Biol. 2008 Jun;10(6):688–97. [PubMed: 18488020]

[39]. Hirata Y, Brotto M, Weisleder N, Chu Y, Lin P, Zhao X, et al. Uncoupling store-operated Ca2+ entry and altered Ca2+ release from sarcoplasmic reticulum through silencing of junctophilin genes. Biophys J. 2006 Jun 15;90(12):4418–27. [PubMed: 16565048]

[40]. Motiani RK, Abdullaev IF, Trebak M. A novel native store-operated calcium channel encoded by Orai3: selective requirement of Orai3 versus Orai1 in estrogen receptor-positive versus estrogen receptor-negative breast cancer cells. J Biol Chem. 2010 Jun 18;285(25):19173–83. [PubMed: 20395295]

[41]. Endo M, Iino M. Properties of calcium release channels of the intracellular calcium store in muscle cells. Adv Second Messenger Phosphoprotein Res. 1990;24:122–7. [PubMed: 2169793]

[42]. Balza RO Jr., Misra RP. Role of the serum response factor in regulating contractile apparatus gene expression and sarcomeric integrity in cardiomyocytes. J Biol Chem. 2006 Mar 10;281(10):6498–510. [PubMed: 16368687]

[43]. Kanakaraj P, Schafer PH, Cavender DE, Wu Y, Ngo K, Grealish PF, et al. Interleukin (IL)-1 receptor-associated kinase (IRAK) requirement for optimal induction of multiple IL-1 signaling pathways and IL-6 production. J Exp Med. 1998 Jun 15;187(12):2073–9. [PubMed: 9625767]

[44]. Beale EG, Hammer RE, Antoine B, Forest C. Disregulated glyceroneogenesis: PCK1 as a candidate diabetes and obesity gene. Trends Endocrinol Metab. 2004 Apr;15(3):129–35. [PubMed: 15046742]

[45]. de Figueiredo LF, Schuster S, Kaleta C, Fell DA. Can sugars be produced from fatty acids? A test case for pathway analysis tools. Bioinformatics. 2009 Jan 1;25(1):152–8. [PubMed: 19117076]

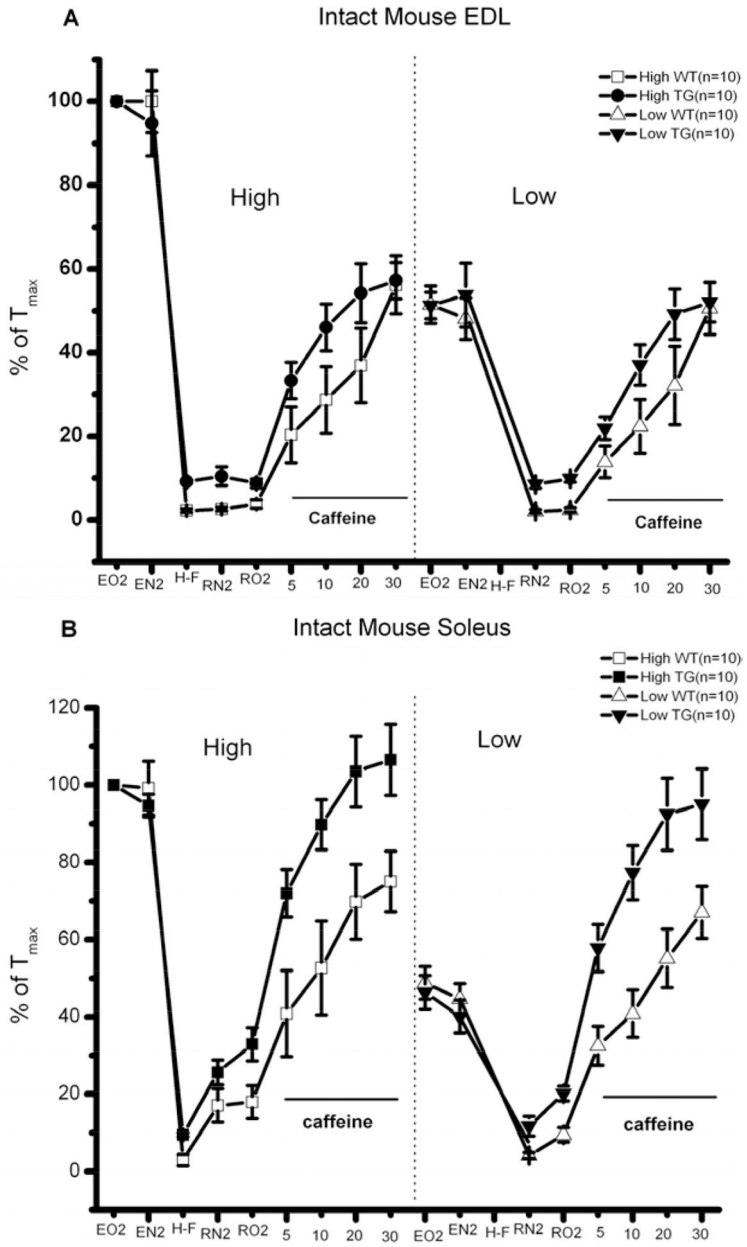

Fig. (1). HSP72 overexpression confers protection to hypoxia-fatigue to EDL and SOL muscles.
A) Intact mouse EDL. **B)** Intact mouse SOL. In general, HSP72 overexpressing muscles fatigued less and displayed significant improved recovery after fatigue, particularly in the presence of caffeine, suggesting enhanced response to CICR.

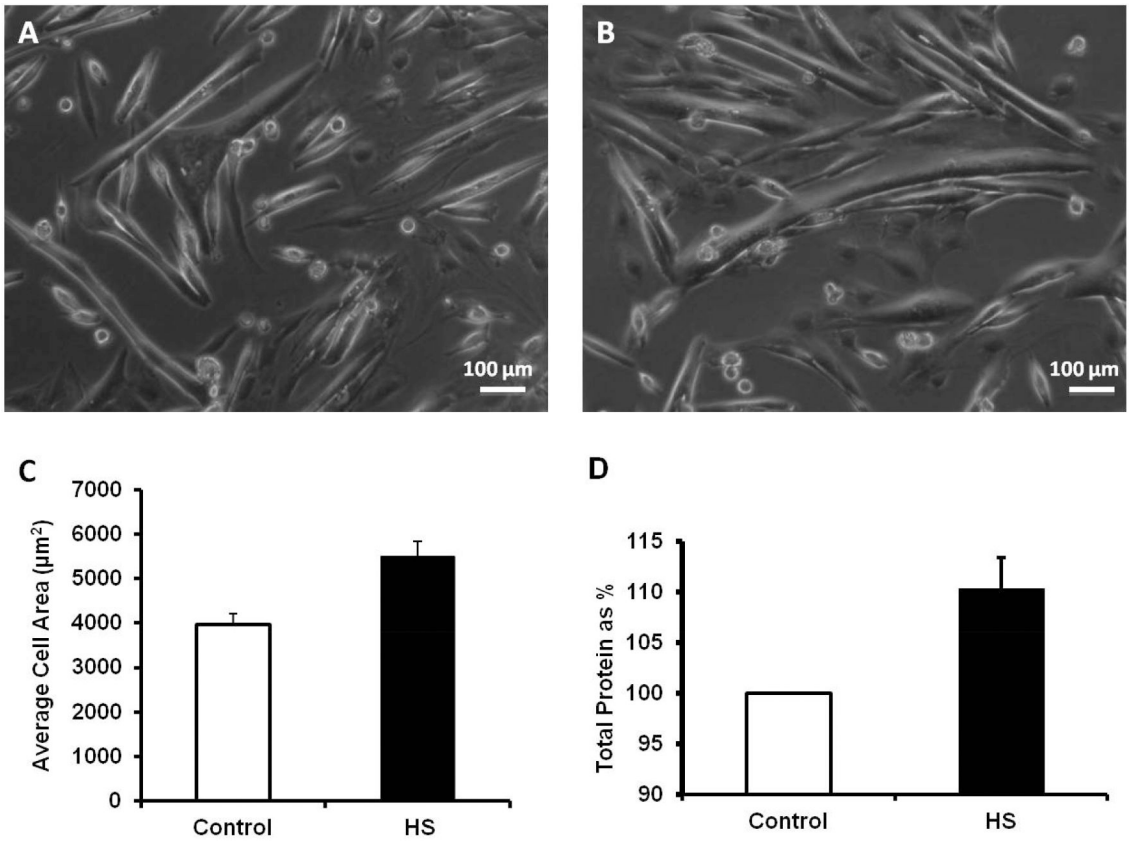

Fig. (2). Heat shock produces a significant increase in the cell area and total protein content in C2C12 myotubes.

All images of C2C12 myotubes were taken with a LEICA DM4000B system equipped with a 14-BIT Snap Cool CCD camera. **A)** Representative images of control C2C12 myotubes. **B)** Representative images of C2C12 myotubes after HS. **C)** Summarized data (mean ± SD) for cell area for control myotubes (n=200) *vs.* HS treated myotubes (n=159), *****P<0.001. **D)** Total protein content is enhanced 24 h after heat-shock treatment (n=5), *****P<0.01.

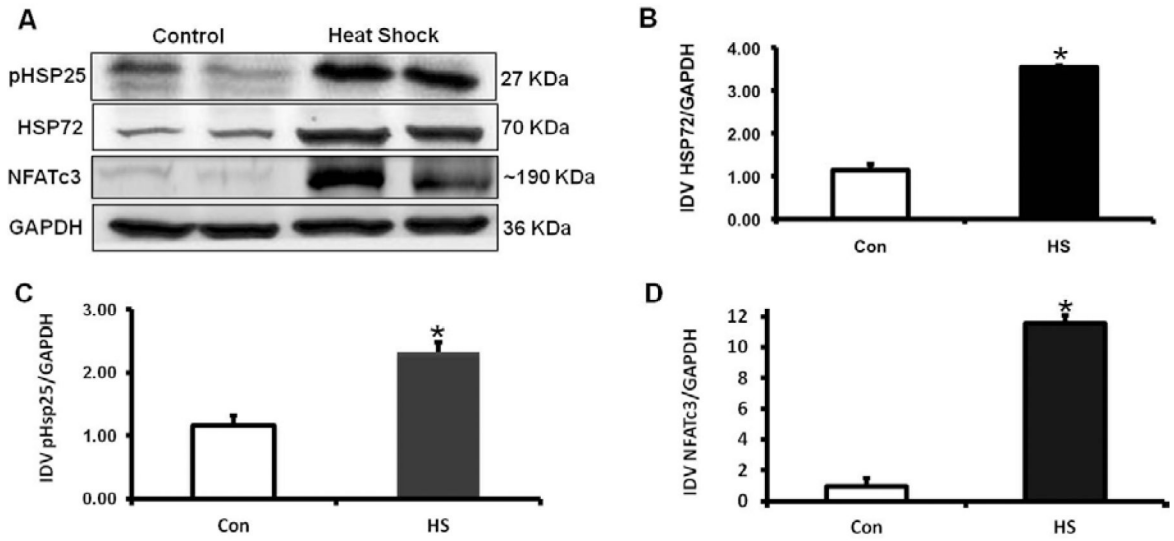

Fig. (3). HS elevates the content of HSP72, enhances the phosphorylation levels of HSP25 and upregulates the Calcineurin/NFATc3 signaling pathway.

A) Representative immunoblot shows the relative levels of HSP72, phosphorylation of HSP25 and NFATc3 in control and HS treated C2C12 myotubes. **B)** Summarized data (means ± SD) for the HSP72/GAPDH ratio, demonstrating the increased content in HSP72 after HS (n=3), *P<0.0035. **C)** Summarized data (mean ± SD) for the p-HSP25/GAPDH ratio, demonstrates that phosphorylation of HSP25 was significantly enhanced by heat-shock (n=3), *P<0.01. **D)** Summarized data (mean ± SD) for the NFATc3/GAPDH ratio, demonstrating the 10-fold increased content in NFATc3 after HS (n=3), *P<0.01. Data is presented as arbitrary units.

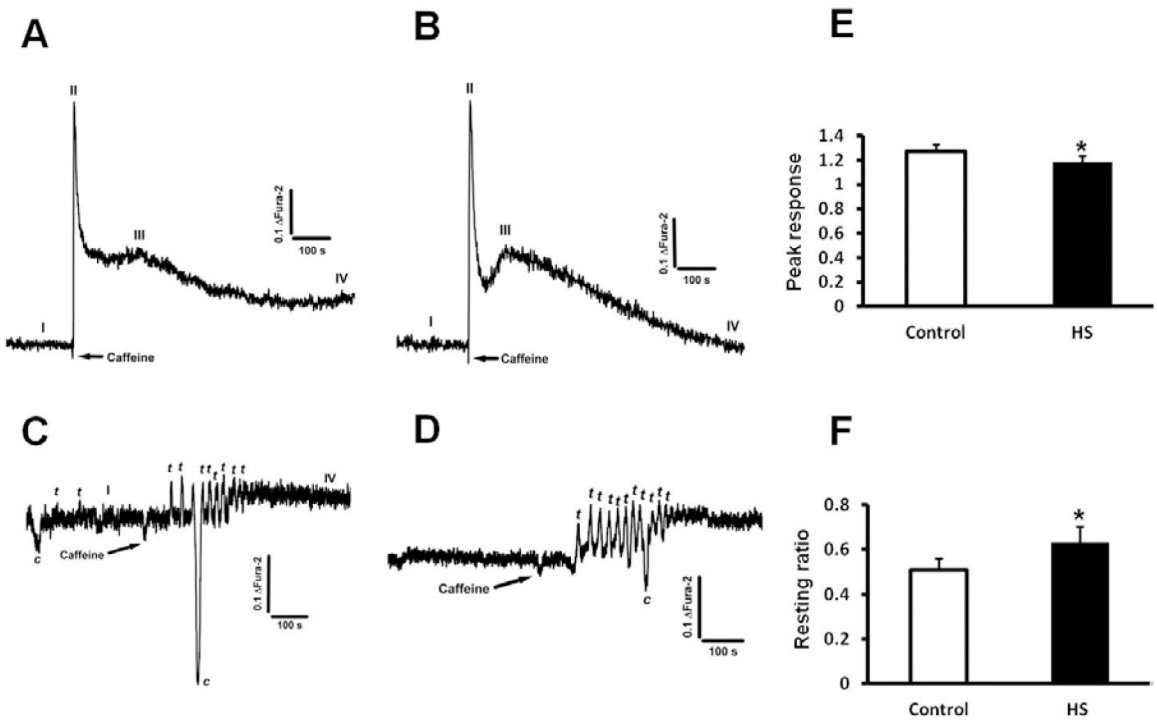

Fig. (4). Intracellular Ca^{2+} homeostasis is modified in C2C12 myotubes after heat-shock treatment.

All panels display Ca^{2+} measurements in fully differentiated C2C12 myotubes normalized as the ratio changes of Fura-2 at excitation wavelengths 350/375 nm and emission at 510 nm. 10mM caffeine was used to trigger Ca^{2+} transients under all conditions tested. I (resting Ca^{2+}), II (caffeine-triggered Ca^{2+} peak), III (second caffeine-triggered Ca^{2+} peak), IV (post-caffeine resting Ca^{2+}) refer to the different parameters systematically observed and measured. The letters *c* and *t* respectively refer to contraction and Ca^{2+} transient. **A)** Representative Ca^{2+} transient in control myotubes, (n=20). **B)** 24 h after HS, C2C12 myotubes have a higher resting level of Ca^{2+}, lower magnitude response after caffeine treatment and display a large second peak in response to caffeine, suggesting enhancement of the CICR response (n=18). **C)** C2C12 myotubes display a very different pattern of response to caffeine 1 h post HS (n=18). The response is initially delayed and then followed by small oscillatory, self-paced Ca^{2+} transients. This pattern is also observed 2 h after HS (n=18) as shown in panel **D**. In most of these cells spontaneous Ca^{2+} transients and muscle cell contractions (recorded as downward deflections in our system) were also common. **E)** Summarized data (mean ± SD) for peak caffeine response in control and 24 h HS cells, and **F)** Summarized data (mean ± SD) for resting ratio in control and 24 h HS cells, *P<0.05 (n=18–20, see for each condition).

Table 1.

Gene PCR Analysis Reveals Molecular Pathways Activated by Heat-Shock in C2C12 Muscle Cells

Group	Subgroup	Gene	20 min*	1h*	2h*	24h*
Heat Shock/ Stress		*Hsp90ab1*	1.3	3.4	6.8	2.6
		Hspa1b (Hsp70)	211	245	301	−1.4
Ca^{+2} signaling	Contractile Machinery	*Jph1*	12.9	−2.4	−7.8	−1.5
		Jph2	1	−3.4	−4.8	−1.3
	SOCE	Orai 3	3.2	−1	−1.9	1.1
		Stim 1	−1	−5.5	−2.3	−1.4
Ca^{+2} release		*RyR1*	−1.2	−1.6	−2.1	−1.9
		IP_3R-1	−1.6	1.2	2.4	1
		IP_3R-3	1	2	3.5	1.4
		Fkbp1b	−1.6	2.9	4.6	3.2
Survival/Metabolic		*Srf*	1.1	1.7	2.2	2.2
		Ppp3r2	1.5	−1.2	4.1	2.6
		Irf1	2.2	1.8	2.2	2.2
		Sod3	1.3	2.3	1.7	−1.8
		Pck1 (Pepck)	1.5	−1.2	2.9	−1
Skeletal Muscle Hypertrophy		*Myh7*	1.2	2.4	4.2	6.8
		Irak	2.8	1	2.8	−1.7
		Traf6	7.6	−1.2	1	−1.2
		Nfkb1	7	1.2	1.7	1.3

Genes are functionally grouped and the genes shown in this table are those essential ones that in our interpretation help explain the molecular pathways leading to the physiological adaptations resulting from HS described in this report.

*fold-change.